IEEE Access
Multidisciplinary | Rapid Review | Open Access Journal

Received 12 September 2022, accepted 3 October 2022, date of publication 21 October 2022, date of current version 28 October 2022.

*Digital Object Identifier 10.1109/ACCESS.2022.3216407*

RESEARCH ARTICLE

# Brain Region-Based Vigilance Assessment Using Electroencephalography and Eye Tracking Data Fusion

**NADIA ABU FARHA[1], FARES AL-SHARGIE[1,2], (Member, IEEE), USMAN TARIQ[1,2], (Member, IEEE), AND HASAN AL-NASHASH[1,2], (Senior Member, IEEE)**

[1]Biomedical Engineering Graduate Program, American University of Sharjah, Sharjah, United Arab Emirates
[2]Department of Electrical Engineering, American University of Sharjah, Sharjah, United Arab Emirates

Corresponding author: Hasan Al-Nashash (hnashash@aus.edu)

This work was supported by the American University of Sharjah under Grant FRG-18-20.

This work involved human subjects or animals in its research. Approval of all ethical and experimental procedures and protocols was granted by the American University of Sharjah's Institutional Review Board (IRB) under Protocol No. 19-513, and performed in line with the Declaration of Helsinki.

**ABSTRACT** Vigilance is the capacity to remain alert for an extended time while performing a task. Staying alert is obligatory in many jobs, particularly those that involve monitoring, such as surveillance tasks, security monitoring, and air traffic control. These monitoring tasks require a specific level of arousal to maintain an adequate level of cognitive efficiency. In this study, we investigate the possibility of assessing the vigilance levels using a fusion of electroencephalography (EEG) and eye tracking data. Vigilance levels were established by performing a modified version of the Stroop color word task (SCWT) for 30 minutes. Feature-level fusion based on the canonical correlation analysis (CCA) was employed to each brain region to improve the classification accuracy of vigilance level assessment. Results obtained using support vector machines (SVM) classifier show that fusion of EEG+eye tracking modalities has improved the classification accuracy compared to individual modality. The EEG+Eye tracking fusion on the right central brain region achieved the highest classification accuracy of 97.4 $\pm$ 1.3%, compared to the individual Beta EEG with 92.0$\pm$ 7.3% and Eye tracking with 76.8$\pm$ 8.4%, respectively. Likewise, EEG and Eye tracking fusion on the right frontal region showed classification accuracy of 96.9 $\pm$ 1.1% for both the Alpha and Beta bands. Meanwhile, when all brain regions were utilized, the highest classification accuracy of EEG+Eye tracking was 96.8 $\pm$ 0.6% using Delta band compared to the EEG alone with 88.18 $\pm$ 8.5% and eye tracking alone with 76.8 $\pm$ 8.4 %, respectively. The overall results showed that vigilance is a brain region specific and the fusion of EEG+ and Eye tracking data using CCA has significantly improved the classification accuracy of vigilance levels assessment.

**INDEX TERMS** Data fusion, EEG, eye tracking, vigilance assessment, canonical correlation analysis (CCA), machine learning.

## I. INTRODUCTION

The ability to pay attention for an extended time is referred to as vigilance [1]. Psychologists and neuroscientists defined the decline in attention-requiring performance over time as vigilance decrement. Vigilance decrement has been identified as a significant risk factor for automobile accidents and a wide range of other crises [2], [3]. Numerous factors contribute to vigilance decrement, including a drop in neuronal stimulation or mental exhaustion affiliated with completing a task for an extended time [4], [5]. There is a growing interest by researchers to minimize the likelihood of errors and accidents. Real-time vigilance level assessment is very critical to avoid the risk of human error in various work

The associate editor coordinating the review of this manuscript and approving it for publication was Vicente Alarcon-Aquino.

environments [6]. In a real-life application, it was reported that stress, work overload, time constraints, and drowsiness all contribute significantly to vigilance decrement [7].

Early studies have established that maintaining vigilant in a stressful environment requires considerable mental workload [8]. Furthermore, studies have demonstrated that while conducting a low-level mental activity, it takes around 30 minutes for target detection performance to drop by 15% [9]. Reduced performance level results in increased reaction time and error rate, both of which can have disastrous results. It has been reported that around 74% of European drivers felt fatigued while driving, which resulted in crashes; rates were lower in Africa (64%), North America (69%), and Asia-Oceania (53%) [5].

The rate at which deterioration in vigilance level happens varies according to the activity. As discussed in [8], tasks can be classified into those that need judgments against a memory value, such as operating a car in a zone with a defined speed limit, and those that require comparative judgments (e.g. oil temperature and oil pressure in an airplane). According to Galy et al. [10], when the workload is described using multidimensional factors, it appears to consist of: 1) Depletion factors on the operator's mental capacity, 2) Mental workload, 3) Performance, and 4) Task intricacy.

Watters et al. [11] suggested that arousal and performance should have a negative quadratic relationship. When an individual is performing a task, the level of interest and engagement gradually increases until the individual achieves optimum performance. However, the performance may deteriorate because of different factors, most notably increased or decreased cognitive workload. Meanwhile, Press et al. [12] reported that factors like fatigue, distraction, boredom, task environment, and external stresses could lead to vigilance decrement. Furthermore, Press et al. [13] linked vigilance decrement to adverse environmental conditions and low motivation caused by a lack of performance feedback.

When physiological data are used to assess cognitive workload, accuracy significantly improves [14], [15]. Vigilance levels fluctuate in response to physiological changes that are regulated by the brain and nervous system. Numerous physiological measures have been utilized to assess cognitive workload. For instance, studies in [16], evaluated seven eye-tracking features to assess mental workload in an experiment involving computerized emergency operating procedures (EOPs) of different levels; the results indicated that the blink rate is task level-dependent, whereas the error rate is arousal level-dependent. Basically, the blink duration increases with prolonged task duration, regardless of task level. Study [17] investigated the accuracy of vigilance level assessment obtained from different classifiers by utilizing six eye tracking features, The pupil size feature showed the highest individual classification accuracy among all the six Eye tracking features. From the same study, a higher accuracy of $76.8 \pm 8.4\%$ was achieved when all the six features were fed to the SVM classifier.

Similarly, another study [18] investigated the operator's work performance in the nuclear power plant (NPP) setting by incorporating two tasks (primary and secondary) and applying both subjective and physiological measures (heart rate variability). The investigation revealed that most participants' heart rates increased when performing high-level tasks. Likewise, study [19] in utilized cerebral blood flow velocity (CBFV) as one of the transcranial doppler sonography (TCD) measurements. The study found that vigilance decrement is accompanied by a decrease in CBFV in the right hemisphere. Another study in [20] investigated the relationship between mental workload and the amount of blood oxygenation in frontal areas, as determined by functional near-infrared spectroscopy (fNIRS). The results revealed the sensitivity of fNIRS measures to mental task load and to the task level.

Meanwhile, study in [21] presented a user-state detection system in an active virtual reality (VR) environment that monitors user behavior using electroencephalography (EEG) via a VR process. The cognitive workload assessment revealed an accuracy of 73.6% and 60.6% for task-levels 0 and 2, respectively. On the other hand, Zarjam et al. [22] compared the detection accuracy using subjective ratings and an EEG-based method with seven different levels of workload. The findings indicated that high task load distinction occurred largely inside the brain's frontal lobe, specifically in the Delta frequency band; this is backed by relevant results stressing the frontal lobe's critical role in managing and performing cognitive tasks due to its close connection to attention and working memory. A 98% detection accuracy was achieved while discriminating seven load levels, compared to the 31% classification accuracy of self-rating. In [23], a system to detect fatigue utilizing EEG was presented for high-speed train safety. The study identified lower frequency components in the forehead region and dispersed them throughout the occipital region during the alert state. A classification accuracy of 90.70% was achieved for driver vigilance detection.

It is critical to assess the vigilance level and monitor it continuously using the best modalities; assessing the vigilance level assists in evaluating the operator's mental state while performing a task [24]. EEG is the most frequently used modality in vigilance assessment. Although EEG has a poor spatial resolution, it remains popular for its high temporal resolution, ease of operation, non-invasive nature, lower cost than other modalities, and ability to record event-related potentials (ERPs) features, which are very useful for studying changes in the human brain over time [25]. In addition to being non-intrusive, the eye tracking approach is regarded as being friendly due to its ease of use. Eye tracking, in addition to EEG, has been shown to improve assessment accuracy [26].

Concerning the fusion approach, [27] developed a data fusion model using electromyogram (EMG) and EEG signals to enhance the vigilance level estimation accuracy. When the individual was asleep, the EEG signals indicated less Beta and Alpha bands power. According to the study, the Beta and Alpha activities decreased as the subject transitioned from awake to sleep. An accuracy of 98-99% was achieved using EEG and EMG, outperforming another study that used simply EEG and achieved 95-96% accuracy [28]. Similarly, [29] utilized a fusion model of hybrid EEG-fNIRS to classify auditory and visual perception; the study achieved an average of 5% improved classification accuracy over single modality classification.

Likewise, Lu et al. [30] enhanced emotion recognition by combining EEG and eye movement using a fuzzy integral fusion strategy. The results showed an accuracy of 87.59%, compared to the individual EEG or the individual eye movement modalities, which had accuracies of 77.80% and 78.51%, respectively. Meanwhile, Rozado et al. [31] combined EEG and pupillometry to assess vigilance levels using mental arithmetic task. For simple arithmetic operations, the fusion produced an error rate of 17%, compared to 26.1% for pupillometry alone and 24.1% for EEG alone. In addition, Kim et al. [32] concatenated the EEG and eye tracking data for cognitive workload assessment. The results indicated a considerable association between cognitive workload metrics based on EEG and eye tracking measurements. Moreover, Bodala et al. [33] assessed cognitive workload level by adopting event related potential (ERP) correlated with micrrosaccades, results showed high correlation of ERP activations to both latency and activation areas.

This study proposes a vigilance level assessment approach by utilizing data fusion of electroencephalography (EEG) and eye tracking. We proposed feature-level fusion using canonical correlation analysis (CCA) as a standardized approach for assessing vigilance levels based on brain region of both the EEG and eye tracking data. In feature level fusion, CCA takes the associated features between two feature vectors as the effective discriminant information, which not only achieves information fusion but also eliminates the redundant features. CCA not only can compress the original feature dimensions but also extract the typical correlation features with good classification performance. Nevertheless, neuroscience studies showed that EEG signals from the same brain region will change similarly during stimulation. The structure and function of each region of interest (ROI) are heterogeneous. In this context, the EEG features from the same ROI would have higher similarity because they exhibit obvious group structures. To obtain more precise correlation, we propose to explore the relationship between intergroup features within different modalities, such as the correlation between the EEG features of one ROI and eye tracking features, with constraints to obtain more discriminative coordinated representations. This can achieve a better detection of vigilance level. To the best of our knowledge, this is the first study on the fusion of EEG features in different scalp regions and eye tracking features from six aspects (pupil size, fixation duration, saccade duration, saccade amplitude, blink duration, and saccade velocity) using CCA.

## II. METHODOLOGY

### A. PARTICIPANTS

Nine healthy students from the American University of Sharjah (age = 24.5 ± 5.5 years) participated in this study. All participants were informed of the experiment's nature, and each participant provided a written informed consent. The experiment was performed between 3.00 P.M - 7:00 P.M to reduce circadian rhythm effects on vigilance and stress levels. Additionally, the experimental protocol was prepared based on the Helsinki declaration and approved by the American University of Sharjah's Institutional Review Board (IRB), the protocol Code 19-513, data of approval 31 March 2020.

### B. VIGILANCE TASK

The nine participants completed a computerized SCWT for thirty minutes [34]. The SCWT task was configured to display six fundamental colors: red, blue, cyan, green, magenta, and yellow. Each time, a word with a specific color was displayed, followed by a random sequence of answers matching the color of the word. The displayed color word did not represent its true meaning, such that the right answer was the word's color, not its meaning (e.g., if cyan is written in red, then red is the correct answer).

The experiment's difficulty level was increased by using random colors for the answering options' background. Reaction time was recorded throughout the training stage to determine the maximum time allowed for each trial. Each trial included a feedback message indicating whether the response was "correct" or "incorrect," in addition to the recorded reaction time. Participants also received a "time is up" feedback message if they did not respond after consuming the trial's allotted time. The SCWT experimental protocol is depicted in Figure 1 with a 45-minute time window [34]. The task length, repetitive nature, and lack of motivation/feedback have triggered vigilance decrement.

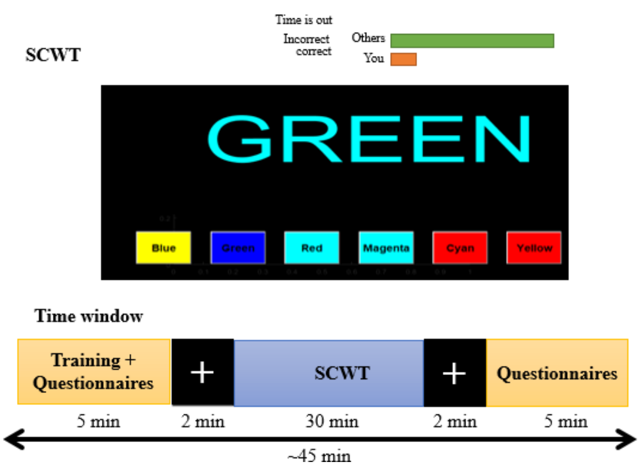


**FIGURE 1.** SCWT presentation interface and time window. The plus symbol with a black background in the time window denotes the pre- and post-baseline periods.

### C. EXPERIMENTAL SETUP AND DATA ACQUISITION

The experiment was conducted at the American University of Sharjah's Biomedical Engineering Laboratory. The lab is a relatively quiet environment in which light and temperature can also be adjusted. The EEG data was acquired at a 500 Hz sampling rate using 64- Ag/AgCl scalp EEG electrodes (ANT Neuro EEG system). Each electrode's impedance was reduced and maintained below 10 KΩ by placing a conductive gel layer between the electrode and the scalp. The system ground was set to the AFz electrode, and the mastoid electrodes M1 and M2 were used to reference the remaining electrodes, as shown in Figure 2. The EyeLink Portable Duo system was used to acquire the eye tracking data at a 500 Hz sampling rate. This system was designed to record non-invasively the gaze position and pupil diameter using an infrared camera. The eye tracking system in our experiment was set to operate in the remote camera mode, which implies that absolute stabilization of the participant's head is unnecessary. In addition, once comfortable with the setup, participants were instructed to minimize their head movement so that their eyes are kept within the eye-tracker's headbox to ensure data quality and continuity. The Eye tracking and EEG data were synchronized by sending markers through the serial and parallel ports triggered by the task events. This was implemented using Matlab with Psychtoolbox. In particular, we sent a marker to the EEG using the parallel port and programmed the Psychtoolbox to send a marker through the serial port.

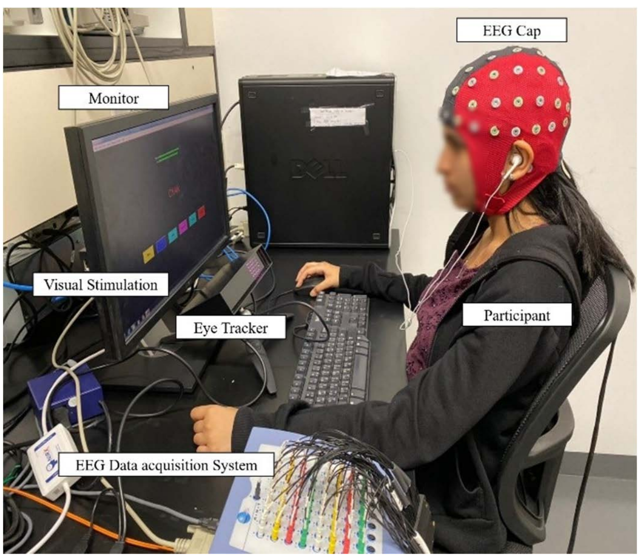


**FIGURE 2.** EEG+Eye tracking data acquisition and experimental set-up.

### D. EEG DATA PREPROCESSING

Preprocessing of the EEG data involved applying a high pass filter at 0.1 Hz to eliminate background signal and DC offset, removing artifacts through independent component analysis (ICA), and applying a 40 Hz low pass filter [35]. Additionally, the EEG channels were re-referenced to all channels average, organized into 1200 ms epochs, and involved a baseline and removal using the whole duration of each epoch. A bandpass filter was used to extract four different frequency bands: Delta (<4 Hz), Theta (4–8 Hz), Alpha (8–13 Hz), and Beta (13–30 Hz).

### E. EYE TRACKING DATA PREPROCESSIN

The following feature extraction was used to provide data preprocessing for eye tracking:

- Baseline adjustment – eliminating all data points from the recording that belong to the first two minutes.
- A minimum of three blink samples are required to establish a blink event.
- Apply extended blinks technique by removing 100 ms before and after a blink event.
- By applying an amplitude threshold of 1.0°, neighboring fixations can be merged.
- Set an onset and offset saccade to verify the 4 ms and 200 ms times; this step prevents saccades from being fragmented into multiple small ones.
- Configure a high pass filter for 30°/s saccade velocity [36], [37], and 0.1° saccade amplitude.
- Develop a histogram for each subject's counts of pupil diameter values.

## III. FEATURE EXTRACTION

### A. EEG DATA FEATURE EXTRACTIO

The power spectral density (PSD) feature was used to analyze the subject's EEG signals. Fast Fourier Transformation (FFT) was employed to perform the EEG data analysis to extract the PSD [38].

### B. EYE TRACKING DATA FEATURE EXTRACTION

The *Data Viewer* software was used to retrieve the eye tracking features; the change in the amplitude of the eye tracking features over time can be used to determine the vigilance levels. Six eye tracking features were retrieved from the eye tracking data gathered in this study: pupil size, fixation duration, saccade duration, saccade amplitude, blink duration, and saccade velocity.

### C. CLASSIFICATION

The support vector machines (SVM) classifier is considered effective for classification and regression analysis. This study employed SVM to distinguish between two vigilance levels: vigilance and vigilance decrement, using clean EEG data, eye tracking and fusion of EEG+Eye tracking data. This classifier has received widespread recognition for its speed, reliability, and high accuracy [39].

## IV. EEG+EYE TRACKING FEATURE LEVEL FUSION

In this study, for each frequency band, the EEG in each trial provided 62 features from the 62 electrodes. On the other hand, the eye tracking data was processed to produce the six features mentioned previously. The two types of vigilance states experienced by subjects during the 30-min

EEG-Eyetracking recordings were based on the behavioral results obtained in an earlier study. We defined the first 5 minutes of the experiment (low reaction time) as the alert state while the last 5 minutes (high reaction time) as the vigilance decrement state. A sliding window of 1 s was used to extract features from the two modalities.

The fusion approach was performed at the feature level. Assume that there are two matrices of features obtained from the two modalities (EEG and eye tracking): $\boldsymbol{A}\in\mathbb{R}^{\boldsymbol{n}\times \boldsymbol{p}}$ and $\boldsymbol{B}\in\mathbb{R}^{\boldsymbol{n}\times \boldsymbol{q}}$, where $\boldsymbol{A}$ and $\boldsymbol{B}$ contain $\boldsymbol{n}$ samples with a $\boldsymbol{p}$ and $\boldsymbol{q}$ feature dimension, respectively. $\boldsymbol{S_{aa}}\in\mathbb{R}^{\boldsymbol{p}\times \boldsymbol{p}}$ and $\boldsymbol{S_{bb}}\in\mathbb{R}^{\boldsymbol{q}\times \boldsymbol{q}}$ denote the correlation matrices of $\boldsymbol{A}$ and $\boldsymbol{B}$, respectively, and $\boldsymbol{S_{ab}}\in\mathbb{R}^{\boldsymbol{p}\times \boldsymbol{q}}$ denotes the covariance matrix, where $\boldsymbol{S_{ab}}=\boldsymbol{S_{ba}^T}$. The canonical correlation (CCA) is then used to obtain $\boldsymbol{A^*} = \boldsymbol{W_a^T A}$ and $\boldsymbol{B^*} = \boldsymbol{W_b^T B}$, which reflect the linear combination of the canonical variates [40], [41]. The canonical variates provide the maximum correlation of shared variance between the two feature sets following Equation (1):

$$\rho(A^*, B^*) = \rho(W_a^T A, W_b^T B) = \frac{W_a^T S_{ab} W_b}{\sqrt{(W_a^T S_{aa} W_a)(W_b^T S_{bb} W_b)}} \tag{1}$$

$\boldsymbol{W_a}$ and $\boldsymbol{W_b}$ are two non-zero arbitrary matrices, where $\boldsymbol{W_a}\in\mathbb{R}^{\boldsymbol{p}}$ and $\boldsymbol{W_b}\in\mathbb{R}^{\boldsymbol{q}}$. The below constraint must be placed to obtain the maximum correlation at which the denominator's two variances are equal to 1:

$$W_a^T S_{aa} W_a = W_b^T S_{bb} W_b = 1 \tag{2}$$

This study's model is summarized in Equation (3); the maximization is calculated by applying the Lagrange multipliers to Equation (1), taking the constraint in Equation (2) into account, and noting that the canonical veritas $\boldsymbol{A}^*$ and $\boldsymbol{B}^*$ are uncorrelated within each data set, with a zero mean and a unit variance. In contrast, the canonical veritas $\boldsymbol{A}^*$ and $\boldsymbol{B}^*$ exhibit a non-zero correlation in their respective indices.

$$Model \begin{cases} \max \rho\left(A^*, B^*\right) \\ W_a^T S_{aa} W_a = W_b^T S_{bb} W_b = 1 \\ W_a \in \mathbb{R}^p, W_b \in \mathbb{R}^q \end{cases} \tag{3}$$

$$\begin{aligned} L\left(A^*, B^*\right) &= L\left(W_a^T A, W_b^T B\right) \\ &= W_a^T S_{ab} W_b - \frac{\lambda_1}{2}\left(W_a^T S_{aa} W_a - 1\right) \\ &\quad - \frac{\lambda_2}{2}\left(W_b^T S_{bb} W_b - 1\right) \end{aligned} \tag{4}$$

where $\lambda_1$ and $\lambda_2$ denote the Lagrange multipliers. Notably, adjusting the partial derivative for $\boldsymbol{L}\left(\boldsymbol{A}^*, \boldsymbol{B}^*\right)$ in Equation (4) with respect $\boldsymbol{W_a}$ and $\boldsymbol{W_b}$ to be equal to zero results in the following two equations:

$$\frac{\partial L}{\partial W_a} = S_{ab} W_b - \lambda_1 S_{aa} W_a = 0 \tag{5}$$

$$\frac{\partial L}{\partial W_b} = S_{ba} W_a - \lambda_2 S_{bb} W_b = 0 \tag{6}$$

Furthermore, by multiplying both sides of the derivative with $\boldsymbol{W_a^T}$ and $\boldsymbol{W_b^T}$ under the condition mentioned in Equation (2), the following result is obtained:

$$W_a^T S_{ab} W_b = \lambda_1 W_a^T S_{aa} W_a = \lambda_1 \tag{7}$$

$$W_b^T S_{ba} W_a = \lambda_2 W_b^T S_{bb} W_b = \lambda_2 \tag{8}$$

Let $\lambda_1 = \lambda_2 = \lambda$, then:

$$\rho(A^*, B^*) = W_a^T S_{ab} W_b = W_b^T S_{ba} W_a = \lambda \tag{9}$$

Equation (9) shows that the Lagrange multipliers $\lambda_1$ and $\lambda_2$ are equal to the correlation coefficients $\boldsymbol{W_a^T}$ and $\boldsymbol{W_b^T}$; notably, substituting the Lagrange multiplier's partial derivative with respect to $\boldsymbol{W_a}$ in the Lagrange multiplier's partial derivative with respect to $\boldsymbol{W_b}$ results in the transformation matrices $\boldsymbol{W_a}$ and $\boldsymbol{W_b}$ using the eigenvalue's equations:

$$S_{aa}^{-1} S_{ab} S_{bb}^{-1} S_{ba} W_a = \lambda^2 W_a \tag{10}$$

$$S_{bb}^{-1} S_{ba} S_{aa}^{-1} S_{ab} W_b = \lambda^2 W_b \tag{11}$$

The eigenvectors are the transformation matrices $\boldsymbol{W_a}$ and $\boldsymbol{W_b}$, while $\boldsymbol{\lambda^2}$ is a vector of eigenvalues or squared canonical correlations. The number of non-zero eigenvalues in each equation is stored in decreasing order. Finally, the final form of fusion is accomplished by concatenating the transformed feature vectors within the corresponding components, as expressed below:

$$F = \begin{pmatrix} A^* \\ B^* \end{pmatrix} = \begin{pmatrix} W_a^T A \\ W_b^T B \end{pmatrix} = \begin{pmatrix} W_a & 0 \\ 0 & W_b \end{pmatrix} \begin{pmatrix} A \\ B \end{pmatrix} \tag{12}$$

where $\boldsymbol{F}$ denotes the canonical correlation discriminant features. From equation (12), the feature vector **F** corresponds to the largest eigenvalues or canonical correlation coefficients. The size of the vector F is the minimum number of data features which is 6 in this study.

The fusion model was employed by utilizing all brain regions at once of a total of 62 electrodes. Additionally, the fusion model was employed for each brain region to investigate the brain region's sensitivity to the change in vigilance level.

Figure 3 shows the framework for this study including data collection by performing the Stroop-color word task from two systems (EEG and Eye tracking). PSD was extracted from the collected EEG data, and the change in the PSD for different brain regions was illustrated using a heat map. On the other hand, the change in the extracted eye tracking features during the two mental states (alertness and VD) was represented by a box plot for each of these features. Data fusion approach based on the canonical correlation analysis was performed followed by a classification approach to determine the accuracy of vigilance level assessment.

## V. RESULTS

### A. EEG VIGILANCE ASSESSMENT LEVEL

The PSD of all subjects was compared using a topographical map under the two mental states: alert and vigilance decrement, for four frequency bands. A topographical map of alertness and vigilance decrement states was constructed for each of the four frequency bands, as well as a topographical map

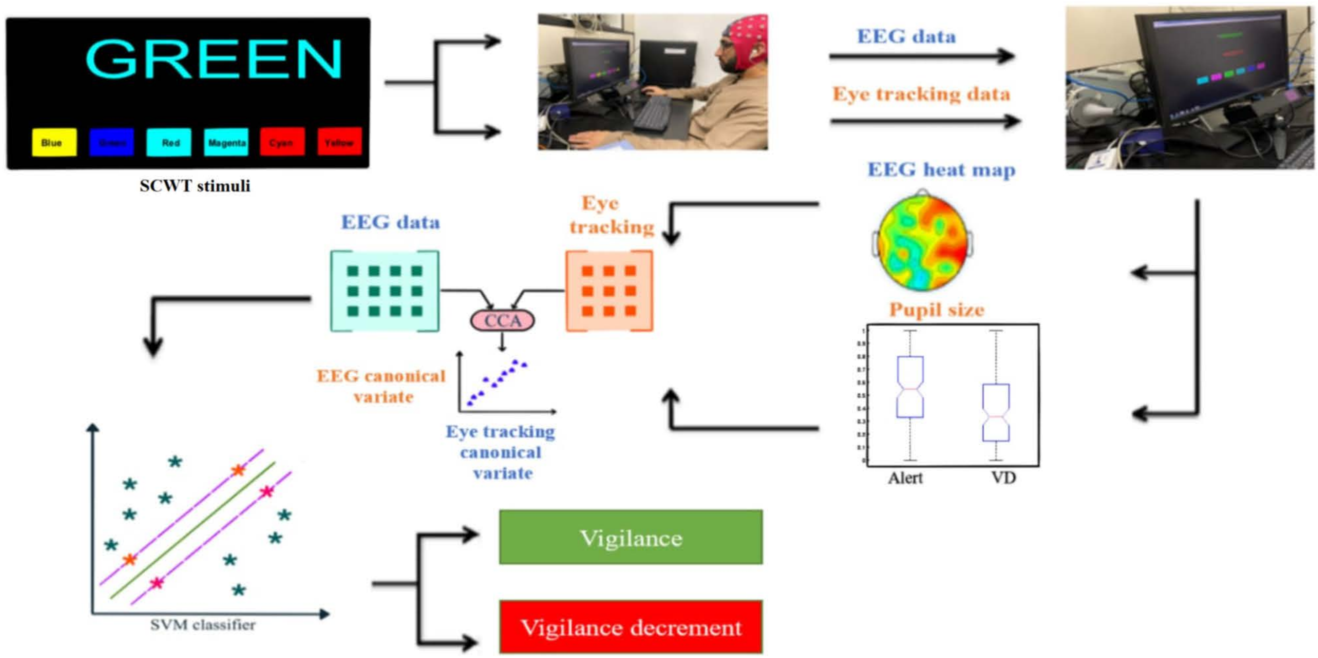


**FIGURE 3.** Experiment processing framework.

based on the t-test between the states as shown in Figure 4. The statistical t-test effectively compared the PSD means for alertness and vigilance decrement; it highlighted the brain regions that were most susceptible to the PSD change the red color indicates highly while blue color indicates less significant differences in vigilance levels. The Statistical t-test topographical map of the Delta and the Alpha bands showed that there was a significant difference in the frontal brain region, the Theta and the Beta bands showed the significant difference in the right temporal and occipital regions. This significant difference in the PSD values reflect the change in the vigilance level between the begging of the task (first 5 minutes of the recording) and the end of it (last 5 minutes of the recording).

The SVM classifier was used to determine the classification accuracy of the vigilance assessment for each of the four EEG frequency bands. We employed a 10-fold cross-validation to estimate the classification accuracy. In this context, feature sets from the alert state and vigilance-decrement state were randomly and evenly split into 10 equally-sized subsets. Nine subsets were used for training and the remaining subset was used for testing, in each iteration. We repeated this procedure 10 times so that each subset is used for validation. TABLE 1 shows that the accuracy of vigilance level assessment for different frequency bands, the highest accuracy obtained was for the Beta band (92.0 ± 7.3%).

### *B. EYE TRACKING VIGILANCE LEVEL ASSESSMENT*

The box plot representation in Figure 5 depicts the mean change in each eye tracking feature and the mean change in all eye tracking features between the alertness and vigilance decrement states. The classification accuracy of the vigilance

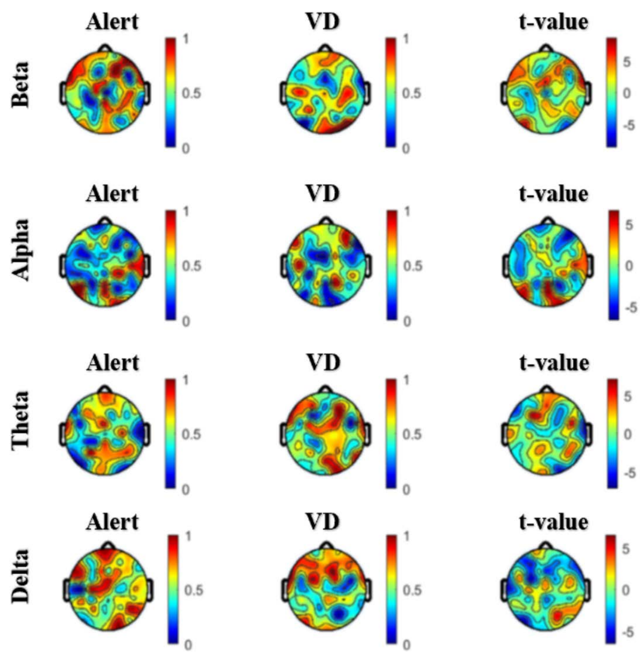


**FIGURE 4.** Comparison of PSD in the four EEG frequency bands across all subjects under the two mental states: alert and vigilance decrement (labeled as VD).

level was determined by feeding the SVM classifiers with six eye tracking features. Moreover, cross-validation was employed to measure the eye tracking vigilance level classification performance. The SVM classifier was used to determine the classification accuracy of the vigilance assessment using the data obtained for six eye tracking features. TABLE 2 showed that the accuracy of vigilance level assessment was the highest for the pupil size (71.8 ± 13.0%). A higher

**TABLE 1.** **EEG bands classification accuracy, specificity, and sensitivity for vigilance assessment.**

| Measure \ Band | Delta | Theta | Alpha | Beta |
|---|---|---|---|---|
| Accuracy | 88.1±8.5% | 81.4±11.2% | 81.5±12.1% | 92.0±7.3% |
| Sensitivity | 86.8±10.3% | 80.1±11.7% | 80.9±13.0% | 91.7±8.0% |
| Specificity | 89.5±7.5% | 82.7±11.3% | 82.2±11.6% | 92.2±7.1% |

**TABLE 2.** **Eye tracking features classification accuracy, sensitivity, and specificity for vigilance assessment.**

| Feature \ Measure | Accuracy | Sensitivity | Specificity |
|---|---|---|---|
| All feature | **76.8±8.4%** | 76.4±11.2% | 77.1±8.5% |
| Fixation duration | 60.9±11.6% | 57.0±12.2% | 64.7±12.5% |
| Pupil size | **71.8±13.0%** | 68.1±15.5% | 75.4±10.9% |
| Saccade duration | 58.8±10.5% | 54.1±11.9% | 63.4±13.1% |
| Saccade amplitude | 57.5±9.6% | 56.3±10.9% | 58.8±9.9% |
| Saccade velocity | 59.3±8.8% | 57.3±13.2% | 61.3±10.3% |
| Blink duration | 56.5±3.1% | 48.9±27.4% | 64.1±26.5% |

classification accuracy obtained when all the six eye tracking features were utilized reaching to 76.8 ± 8.4%.

### C. DATA FUSION VIGILANCE LEVEL ASSESSMENT

The extracted feature matrices from the EEG and eye tracking were utilized as inputs for the fusion; this fusion approach helped explore the correlation between EEG and eye tracking data in different frequency bands. The mean correlation coefficient values obtained from EEG+eye tracking were displayed alongside a heat map for the cross-subject correlation matrix for each of the four frequency bands as shown in Figure 6.

The selection criteria considered the components' correlation level extracted from the modified feature vectors, where components with small canonical correlations were discarded. CCA was applied to the entire data set arranged in descending rank order to obtain the canonical correlations of the eye tracking and EEG features for vigilance assessment. The estimated joint covariance matrix was used to compute these canonical correlations. The results of the correlation coefficients when all brain regions were utilized are shown in Figure 6 and TABLE 3 illustrates the correlation coefficients for fusing each brain (right(R), left (L)) separately.

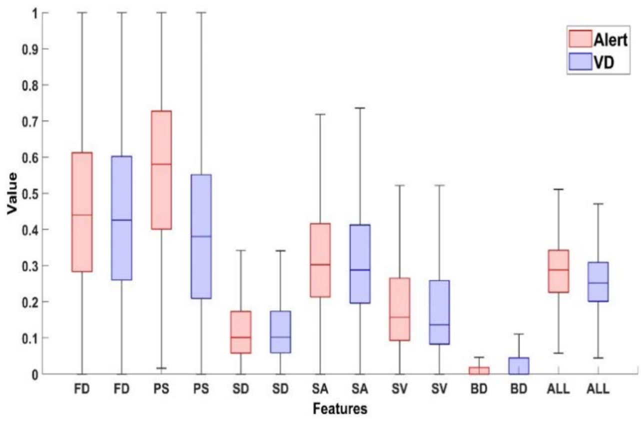


**FIGURE 5.** **Mean change for individual eye tracking features [Fixation Duration (FD), Pupil Size (PS), Saccade Duration (SD), Saccade Amplitude (SA), Saccade Velocity (SV), Blink Duration (BD)], and all features (ALL) between alertness and vigilance decrement.**

Figure 6 shows that the correlation varies with the components used, where the components of the x-axis refer to the six EEG+eye tracking features. Therefore, the higher the correlation value, indicates a higher change in vigilance level. In addition, the cross-subject source correlation matrix

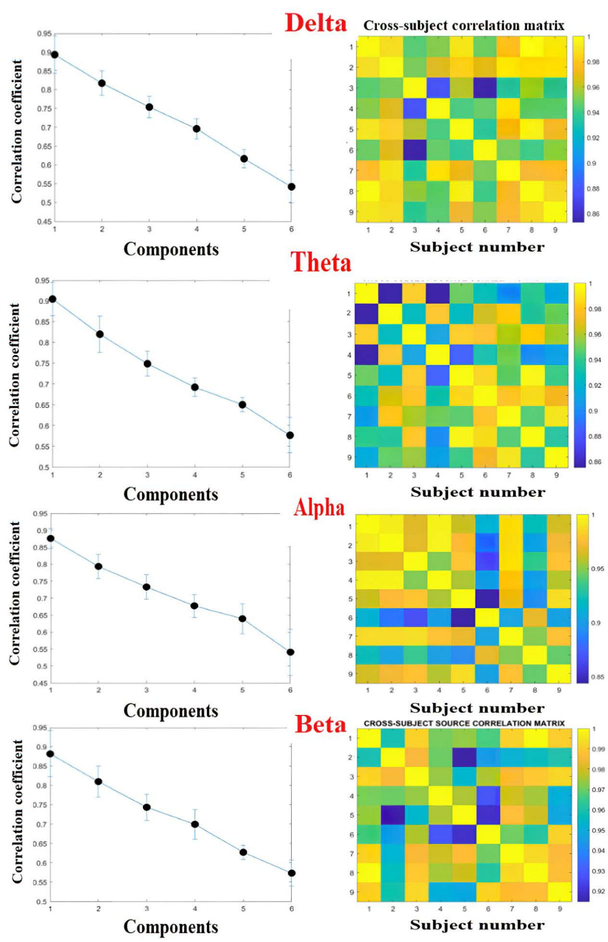


**FIGURE 6.** **Correlation coefficient values for the EEG-eye tracking CCA, and the cross-subject correlation heat map per EEG frequency band.**

**TABLE 3.** Mean value of the correlation coefficients for the brain region-based EEG-Eye tracking CCA.

| Region | | Delta | Theta | Alpha | Beta |
|---|---|---|---|---|---|
| Frontal | R | 0.4361 | 0.4537 | 0.4381 | 0.4500 |
| | L | 0.4359 | 0.4341 | 0.4506 | 0.4688 |
| Temporal | R | 0.4192 | 0.4914 | 0.4377 | 0.4797 |
| | L | 0.4418 | 0.4197 | 0.4397 | 0.4593 |
| Central | R | 0.5028 | 0.5309 | 0.4870 | 0.5274 |
| | L | 0.5220 | 0.5159 | 0.5260 | 0.5227 |
| Parietal | R | 0.4206 | 0.4408 | 0.4522 | 0.4649 |
| | L | 0.3958 | 0.4006 | 0.4348 | 0.4645 |
| Occipital | R | 0.4129 | 0.4417 | 0.4471 | 0.4610 |
| | L | 0.4290 | 0.4071 | 0.3953 | 0.4258 |

is determined by calculating the correlation coefficients of the subjects and then averaging the correlation coefficients across all. The matrix represented by the heat map shows the consistency in inter-subject correlation between the two modalities.

The classification accuracy, sensitivity, and specificity were obtained using the SVM classifier when data from every EEG frequency band were fused with the six eye tracking data to evaluate the vigilance level. Classification accuracy was attained by fusing all brain regions as shown in TABLE 4.

**TABLE 4.** EEG-eye tracking fusion classification accuracy, sensitivity, and specificity for vigilance assessment.

| Measure \ Band | Delta-eye tracking fusion | Theta-eye tracking fusion | Alpha-eye tracking fusion | Beta-eye tracking fusion |
|---|---|---|---|---|
| Accuracy | 96.8±0.6% | 96.1±1.1% | 96.3±1.1% | 96.8±1.1% |
| Sensitivity | 97.3±1.0% | 97.0±1.2% | 97.0±1.1% | 97.2±1.0% |
| Specificity | 96.3±0.9% | 95.2±1.3% | 95.7±1.6% | 96.4±1.2% |

A box plot was generated to illustrate the $p$-value determined using the paired sample t-test for the classification accuracy obtained for each of the EEG and eye tracking in comparison with the fusion of them. The $p$-value shows significant difference between the accuracies obtained using the individual EEG modality and the accuracies obtained using the fusion model (EEG+Eye tracking) for four frequency bands.

From TABLE 5, region based fusion model for the EEG and the eye tracking showed that the right central brain region was the most sensitive region to vigilance with an accuracy of 97.4±1.3% in the Beta band, followed by a close classification accuracy of 96.9±1.1% in both Beta and Alpha bands in the right frontal region.

## VI. DISCUSSION

This study aimed to investigate the accuracy of adopting the EEG or eye tracking for vigilance assessment. Additionally, the fusion of bimodality (EEG-eye tracking) was examined whether it could enhance vigilance assessment. The adopted approach collected data from nine subjects while simultaneously measuring their EEG and eye tracking. The data fusion model was first applied to all brain regions and then to individual ones. The EEG results indicated that the Beta band provided the highest classification accuracy of 92.0 ± 7.3%, followed by the Delta band with a close accuracy of 88.1 ± 8.5%. Meanwhile, Alpha and Theta provided the lowest classification accuracy for vigilance assessment between the alertness and vigilance decrement states.

Beta waves are associated with alertness and normal waking consciousness [42], [43]. The Beta range of human EEG signals is highly connected with the analysis of different cognitive processes like recognition tasks and informational differentiation processes [44]. Moreover, the Delta wave is associated with sleep, deep sleep, and the unconscious state. According to [45], the Delta frequency band has a main role in carrying most of the information related to working memory load since it appeared to be tied to the subjects' concentration increment during the experiment. With its low-frequency activity, the Delta EEG band exhibited significant electrophysiological correlations with cognitive processing and should receive more attention in future studies.

Beta and Delta bands were shown to be the most sensitive to changes in the vigilance level in this study due to their strong association with either alertness. The SCWT

**TABLE 5. EEG-eye tracking brain region based fusion classification accuracy, sensitivity, and specificity for vigilance assessment.**

| Brain region | Band / Measure | Delta | Theta | Alpha | Beta |
|---|---|---|---|---|---|
| Right frontal | Accuracy | **96.6±1.3** | 96.4±1.3 | 96.9±1.1 | 96.9±1.1 |
| | Sensitivity | 97.2±1.1 | 96.8±1.1 | 97.4±1.1 | 97.4±1.2 |
| | Specificity | 96.0±1.6 | 95.9±1.8 | 96.3±1.3 | 96.3±1.3 |
| Left frontal | Accuracy | **96.9±1.5** | 95.5±1.3 | 96.4±1.0 | 96.7±1.6 |
| | Sensitivity | 97.5±1.4 | 96.2±1.8 | 97.4±0.8 | 97.6±1.6 |
| | Specificity | 96.2±1.9 | 94.8±1.5 | 95.4±1.5 | 95.8±2.2 |
| Right temporal | Accuracy | 93.4±2.5 | 92.8±2.9 | 92.4±3.2 | **94.8±2.2** |
| | Sensitivity | 95.2±2.2 | 94.1±2.0 | 94.5±2.5 | 96.7±1.7 |
| | Specificity | 91.7±3.02 | 91.5±3.1 | 90.4±4.4 | 92.8±3.0 |
| Left temporal | Accuracy | 93.7±3.0 | 92.6±2.2 | 93.3±1.7 | **94.9±3.2** |
| | Sensitivity | 95.5±2.0 | 94.5±1.8 | 95.3±1.6 | 96.4±2.2 |
| | Specificity | 91.0±4.4 | 90.8±2.8 | 91.3+-2.6 | 93.4±4.4 |
| Right central | Accuracy | 96.2±1.3 | 96.6±1.4 | 96.5±1.49 | **97.4±1.3** |
| | Sensitivity | 97.2±1.1 | 97.0±1.3 | 97.5±1.1 | 97.9±1.4 |
| | Specificity | 95.2±1.8 | 96.2±1.8 | 95.4±2.0 | 96.9±1.3 |
| Left central | Accuracy | 96.7±1.1 | 95.6±1.5 | 96.8±1.2 | **97.2±1.3** |
| | Sensitivity | 97.7±1.0 | 96.4±1.3 | 97.6±1.1 | 97.8±0.9 |
| | Specificity | 95.7+-1.7 | 94.8±2.1 | 96.0±1.4 | 96.5±2.0 |
| Right parietal | Accuracy | 94.8±2.5 | 95.0±1.8 | 95.5±1.9 | **96.7±2.1** |
| | Sensitivity | 96.2±2.0 | 96.1±1.8 | 96.8±1.4 | 97.7±1.3 |
| | Specificity | 93.4±3.5 | 94.0±1.9 | 94.2±2.6 | 95.8±3.1 |
| Left parietal | Accuracy | 94.2±2.3 | 94.7±2.2 | 95.3±2.4 | **96.0±2.2** |
| | Sensitivity | 95.7±2.0 | 96.0±1.9 | 96.6±1.9 | 97.1±1.8 |
| | Specificity | 92.6±3.0 | 93.3±2.8 | 93.9±3.0 | 95.0±3.0 |
| Right occipital | Accuracy | 93.1±2.6 | 93.6±2.4 | 93.0±3.5 | **93.9±3.1** |
| | Sensitivity | 94.8±2.2 | 95.0±2.3 | 95.5±2.4 | 95.4±2.1 |
| | Specificity | 91.5±3.3 | 92.3±3.2 | 90.5±4.8 | 92.4±4.2 |
| Left occipital | Accuracy | **93.2±2.5** | 92.3±2.6 | 92.4±3.3 | 93.1±3.0 |
| | Sensitivity | 95.1±2.0 | 94.4±2.0 | 95.0±3.3 | 95.3±2.0 |
| | Specificity | 91.3±3.3 | 90.3±3.3 | 89.8±4.3 | 90.8±4.3 |

requires great attention to color recognition and a high memory strength to respond quickly and minimize reaction time.

Using a topographical map, Figure 4 illustrates a significant PSD change across some brain areas between alertness states and vigilance decrement for all four EEG frequency bands. Notably, the occipital and frontal brain regions were the most sensitive to vigilance decrement. The occipital brain region is associated with visual activity processing, memory formation, distance, and depth perception; it is also assumed to be responsible for color determination. On the other hand, the frontal brain region is involved in high-level cognitive functions, including emotions, memory, impulse control, social interaction, problem-solving, and motor function [46]. The topographical map corroborated the EEG classification, as both Beta and Delta waves were captured in the brain's frontal lobes [47].

Likewise, when six eye tracking features were utilized, the eye tracking data showed a lower classification accuracy for vigilance assessment at 76.8 ± 8.4%. A possible justification for the low accuracy is that the eye tracking system is very sensitive and has a limitation that needs the subject's eye to be stationary and on-axis with regard to the eye tracking camera. Moreover, eye tracking features are highly sensitive to light; light control using the same features can enhance classification accuracy [48]. A comparison of all six eye tracking features was conducted to determine the relative importance of each feature in vigilance assessment. The results revealed that the pupil size provided the highest classification accuracy (71.8 ± 13.0%). Numerous studies have reported high classification accuracy when the pupil size feature is used [49], [50]. The box plot in Figure 5 compares the mean change in eye tracking features for alertness and vigilance decrement, revealing that vigilance decrement appeared to have less spread and a lower mean than alertness.

A feature level fusion was employed by grouping the temporal information of features for two modalities (EEG and eye tracking). The proposed fusion approach was based on CCA - a prevalent method to explore the correlation between two modalities [51], [41]. CCA is well-known as a powerful and versatile tool for finding relationships between different data types. It also helps eliminate feature redundancy and provides a feature vector with effective discriminant information [52]. Since EEG and eye tracking data are dissimilar in nature, it is very hard to analyze both types together. Therefore, fusing the data using CCA helped reduce both modalities to a single feature corresponding to alertness and vigilance decrement.

The associations across these feature datasets were then explored by leveraging the inter-subject covariations to assess the connection between the two modalities [53], [54]. As shown in Table 3, fusion improved the accuracy of all EEG bands; the Delta band acquired the highest fusion accuracy of 96.8 ± 0.6% when all brain regions were included

(62 electrodes). All other bands obtained a close fusion accuracy to Delta. Furthermore, the Delta band appeared to be the most sensitive to vigilance decrement. Thus, the data fusion results were relevant to this study's expectations, as this band is associated with the deepest level of relaxation.

A possible explanation for the discrepancy between the increases in Delta waves during the SCWT task is the presence of an inhibition that is activated during a mental task to suppress irrelevant or inappropriate neural activities selectively [55]. Although, little emphasis was placed on low frequencies in assessing cognitive workload, study in [56] reported that the Delta band is associated with cognitive processes involved with attention, detection of motivationally salient environmental cues, and behavioral inhibition. On the other hand, [57] asserted that the oscillation of the brain's electric field determines the neural pool involved; this could explain why Delta wave oscillations may have a significant role in cognitive workload processing. According to the study, neural networks located beyond the frontal lobes might be modulated by Delta, produced in the frontal cortex during mental tasks.

The fusion model based on brain region showed that the right central brain region was the most sensitive region to vigilance with an accuracy of 97.4±1.3% in the Beta band, followed by a close classification accuracy of 96.9±1.1% in both Beta and Alpha bands in the right frontal region. The accuracy gained based on the brain region was slightly higher than when all regions were utilized. The results supported that the central and frontal brain regions are highly sensitive to the vigilance level. According to [58], the central brain region exhibits one of the highest correlations between cognitive workload and EEG features in Beta waves. Besides, [59] confirmed that both frequency bands alpha and theta showed less power in central and posterior regions when the difficulty level increased. Additionally, [60] obtained a completely different EEG pattern for assessing cognitive workload, with an increase in power in either hemisphere's orbitofrontal and central areas, as well as left temporal regions. Similarly, [61] reported that when EEG signals based on entropy features were used for cognitive workload assessment, an accuracy of 98% was achieved for channels from the frontal lobes.

Another fusion model demonstrated that the vigilance level is predominantly tied to the Beta activity in the brain's central and frontal regions of the brain; besides, the study reported that there were no substantial differences between the left and right hemispheres, as also reported by other studies [62].

In addition to showing the p-value calculated using the paired sample t-test, a box plot classification accuracy obtained for the EEG and the eye tracking is shown in Figure 7. A significant difference appeared between the EEG Delta band and the fusion using the EEG Delta band (F-D) with a $p < 0.01$. The same result was obtained for the Theta and Alpha bands. On the other hand, the Beta band demonstrated a difference of $p = 0.06$ between utilizing it alone and through the proposed fusion approach (F-B). These results imply that CCA enhances accuracy significantly. Although,

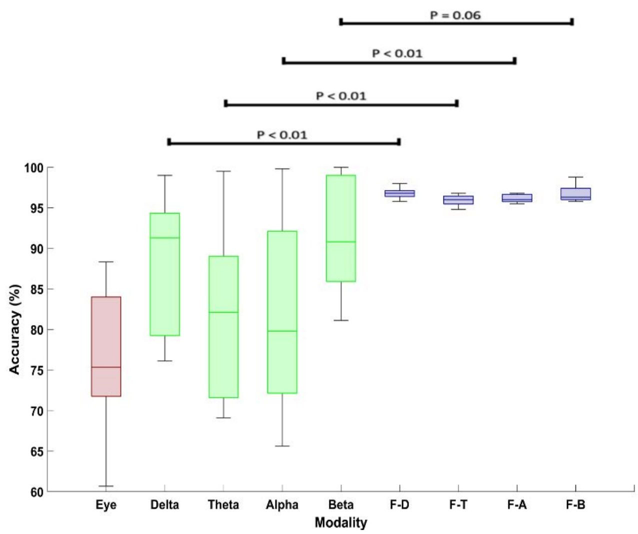


**FIGURE 7.** Box plot of classification accuracies obtained for the EEG and eye tracking data, as well as CCA fusion. The paired sample t-test was used to calculate p-values. F-T, F-D, F-A, and F-B denote data fusion using the Theta band, Delta band, Alpha band, and Beta band, respectively.

we have achieved high classification accuracy using CCA, decision level fusion is worth investigating to compare the results and support our finding.

## VII. CONCLUSION

This study employed a fusion strategy, combining eye tracking and EEG technology for vigilance assessment based on the brain region. The vigilance assessment was based on a feature-level fusion of both EEG and eye tracking features using CCA. The results indicated that the fusion improved the classification accuracy of both modalities. The EEG Delta band achieved the highest accuracy for the fusion at 96.8 ± 0.6%, higher than the EEG Delta band without fusion (88.18 ± 8.5%) or the eye tracking data alone (76.8 ± 8.4%) when all brain regions were involved. Higher fusion accuracy was also obtained in the right central region of (97.4 ± 1.3%) of the Beta band. Moreover, high accuracy of 96.9 ± 1.1% was achieved in the right frontal region for the Beta and Alpha activities. In the future research, we will consider other features rather than PSD for vigilance level assessment, study [5] proved that connectivity patterns and graph theory analysis are very informative features that have been utilized for vigilance assessment. These features are worth investigation using a data fusion approach that utilizes the connectivity patterns and the eye tracking data to enhance the classification accuracy obtained for vigilance assessment.

## REFERENCES

[1] L. C. Reteig, R. L. van den Brink, S. Prinssen, M. X. Cohen, and H. A. Slagter, "Sustaining attention for a prolonged period of time increases temporal variability in cortical responses," *Cortex*, vol. 117, pp. 16–32, Aug. 2019, doi: 10.1016/j.cortex.2019.02.016.

[2] C. Sauter, H. Danker-Hopfe, E. Loretz, J. Zeitlhofer, P. Geisler, and R. Popp, "The assessment of vigilance: Normative data on the siesta sustained attention test," *Sleep Med.*, vol. 14, no. 6, pp. 542–548, Jun. 2013, doi: 10.1016/j.sleep.2013.01.011.

[3] I. P. Bodala, Y. Ke, H. Mir, N. V. Thakor, and H. Al-Nashash, "Cognitive workload estimation due to vague visual stimuli using saccadic eye movements," in *Proc. 36th Annu. Int. Conf. IEEE Eng. Med. Biol. Soc.*, Aug. 2014, pp. 2993–2996, doi: 10.1109/EMBC.2014.6944252.
[4] B. W. Y. Hornsby, G. Naylor, and F. H. Bess, "A taxonomy of fatigue concepts and their relation to hearing loss," *Ear Hearing*, vol. 37, pp. 136–144, Jul. 2016, doi: 10.1097/AUD.0000000000000289.
[5] F. Al-shargie, U. Tariq, H. Mir, H. Alawar, F. Babiloni, and H. Al-nashash, "Vigilance decrement and enhancement techniques: A review," *Brain Sci.*, vol. 9, no. 8, p. 178, Jul. 2019, doi: 10.3390/brainsci9080178.
[6] L. K. McIntire, R. A. McKinley, C. Goodyear, and J. P. McIntire, "Detection of vigilance performance using eye blinks," *Appl. Ergonom.*, vol. 45, no. 2, pp. 354–362, Mar. 2014, doi: 10.1016/j.apergo.2013.04.020.
[7] F. Sauvet, C. Bougard, M. Coroenne, L. Lely, P. Van Beers, M. Elbaz, M. Guillard, D. Leger, and M. Chennaoui, "In-flight automatic detection of vigilance states using a single EEG channel," *IEEE Trans. Biomed. Eng.*, vol. 61, no. 12, pp. 2840–2847, Dec. 2014, doi: 10.1109/TBME.2014.2331189.
[8] J. S. Warm, R. Parasuraman, and G. Matthews, "Vigilance requires hard mental work and is stressful," *Hum. Factors*, vol. 50, no. 3, pp. 433–441, 2008, doi: 10.1518/001872008X312152.
[9] N. Pattyn, X. Neyt, D. Henderickx, and E. Soetens, "Psychophysiological investigation of vigilance decrement: Boredom or cognitive fatigue?" *Physiol. Behav.*, vol. 93, nos. 1–2, pp. 369–378, Jan. 2008, doi: 10.1016/j.physbeh.2007.09.016.
[10] E. Galy and C. Mélan, "Effects of cognitive appraisal and mental workload factors on performance in an arithmetic task," *Appl. Psychophysiol. Biofeedback*, vol. 40, no. 4, pp. 313–325, Dec. 2015, doi: 10.1007/s10484-015-9302-0.
[11] P. A. Watters, F. Martin, and Z. Schreter, "Caffeine and cognitive performance: The nonlinear Yerkes–Dodson law," *Hum. Psychopharmacol.*, vol. 12, no. 3, pp. 249–257, 1997, doi: 10.1002/(SICI)1099-1077(199705/06)12:3<249::AID-HUP865>3.0.CO;2-J.
[12] R. R. Mackie, "Vigilance: Theory, operational performance, and physiological correlates," *Aviation Space Environ. Med.*, vol. 91, no. 3, pp. 550–552, 2020.
[13] D. R. Davies and R. Parasuraman, "The psychology of vigilance," *Amer. J. Psychol.*, vol. 97, no. 3, pp. 466–467, 1984.
[14] S. Yang, S. A. R. Hosseiny, S. Susindar, and T. K. Ferris, "Investigating driver sympathetic arousal under short-term loads and acute stress events," in *Proc. Hum. Factors Ergonom. Soc. Annu. Meeting*, 2016, p. 1898, doi: 10.1177/1541931213601434.
[15] X. Fan, "Emotion recognition from physiological signals," in *Proc. 13th Int. Symp. Comput. Intell. Design*, 2020, pp. 81–86, doi: 10.1109/ISCID51228.2020.00025.
[16] Q. Gao, Y. Wang, F. Song, Z. Li, and X. Dong, "Mental workload measurement for emergency operating procedures in digital nuclear power plants," *Ergonomics*, vol. 56, no. 7, pp. 1070–1085, Jul. 2013, doi: 10.1080/00140139.2013.790483.
[17] N. A. Farha, F. Al-Shargie, U. Tariq, and H. Al-Nashash, "Artifact removal of eye tracking data for the assessment of cognitive vigilance levels," in *Proc. 6th Int. Conf. Adv. Biomed. Eng. (ICABME)*, Oct. 2021, pp. 175–179, doi: 10.1109/ICABME53305.2021.9604870.
[18] S.-L. Hwang, Y.-J. Yau, Y.-T. Lin, J.-H. Chen, T.-H. Huang, T.-C. Yenn, and C.-C. Hsu, "Predicting work performance in nuclear power plants," *Saf. Sci.*, vol. 46, no. 7, pp. 1115–1124, Aug. 2008, doi: 10.1016/j.ssci.2007.06.005.
[19] T. H. Shaw, J. S. Warm, V. Finomore, L. Tripp, G. Matthews, E. Weiler, and R. Parasuraman, "Effects of sensory modality on cerebral blood flow velocity during vigilance," *Neurosci. Lett.*, vol. 461, no. 3, pp. 207–211, Sep. 2009, doi: 10.1016/j.neulet.2009.06.008.
[20] H. Ayaz, P. A. Shewokis, S. Bunce, K. Izzetoglu, B. Willems, and B. Onaral, "Optical brain monitoring for operator training and mental workload assessment," *NeuroImage*, vol. 59, no. 1, pp. 36–47, Jan. 2012, doi: 10.1016/j.neuroimage.2011.06.023.
[21] C. Tremmel, C. Herff, T. Sato, K. Rechowicz, Y. Yamani, and D. J. Krusienski, "Estimating cognitive workload in an interactive virtual reality environment using EEG," *Frontiers Hum. Neurosci.*, vol. 13, p. 401, Nov. 2019, doi: 10.3389/fnhum.2019.00401.
[22] P. Zarjam, J. Epps, and N. H. Lovell, "Beyond subjective self-rating: EEG signal classification of cognitive workload," *IEEETrans. Auton. Mental Develop.*, vol. 7, no. 4, pp. 301–310, Dec. 2015, doi: 10.1109/TAMD.2015.2441960.
[23] X. Zhang, J. Li, Y. Liu, Z. Zhang, Z. Wang, D. Luo, X. Zhou, M. Zhu, W. Salman, G. Hu, and C. Wang, "Design of a fatigue detection system for high-speed trains based on driver vigilance using a wireless wearable EEG," *Sensors*, vol. 17, no. 3, p. 486, 2017, doi: 10.3390/s17030486.
[24] M. Lohani, B. R. Payne, and D. L. Strayer, "A review of psychophysiological measures to assess cognitive states in real-world driving," *Frontiers Hum. Neurosci.*, vol. 13, pp. 1–27, Mar. 2019, doi: 10.3389/fnhum.2019.00057.
[25] A. M. Beres, "Time is of the essence: A review of electroencephalography (EEG) and event-related brain potentials (ERPs) in language research," *Appl. Psychophysiol. Biofeedback*, vol. 42, no. 4, pp. 247–255, Dec. 2017, doi: 10.1007/s10484-017-9371-3.
[26] A. Sahayadhas, K. Sundaraj, and M. Murugappan, "Detecting driver drowsiness based on sensors: A review," *Sensors*, vol. 12, no. 12, pp. 16937–16953, Dec. 2012, doi: 10.3390/s121216937.
[27] M. Akin, M. B. Kurt, N. Sezgin, and M. Bayram, "Estimating vigilance level by using EEG and EMG signals," *Neural Comput. Appl.*, vol. 17, no. 3, pp. 227–236, Jun. 2008, doi: 10.1007/s00521-007-0117-7.
[28] M. Akin, O. Erogul, M. Bayram, and N. Sezgin, "Determining of doze level analysing EEG signals by using wavelet transform and neural networks," in *Proc. Int. 12th Turkish Symp. Artif. Intell. Neural Netw. (TAINN)*, 2003, pp. 1–7.
[29] F. Putze, S. Hesslinger, C.-Y. Tse, Y. Huang, C. Herff, C. Guan, and T. Schultz, "Hybrid fNIRS-EEG based classification of auditory and visual perception processes," *Frontiers Neurosci.*, vol. 8, pp. 1–13, Nov. 2014, doi: 10.3389/fnins.2014.00373.
[30] Y. Lu, W. L. Zheng, B. Li, and B. L. Lu, "Combining eye movements and EEG to enhance emotion recognition," in *Proc. 24th Int. Joint Conf. Artif. Intell.*, 2015, pp. 1170–1176.
[31] D. Rozado and A. Dünser, "Combining EEG with pupillometry to improve cognitive workload detection," *Computer*, vol. 48, no. 10, pp. 18–25, Oct. 2015, doi: 10.1109/MC.2015.314.
[32] J.-H. Kim, D.-W. Kim, and C.-H. Im, "Brain areas responsible for vigilance: An EEG source imaging study," *Brain Topography*, vol. 30, no. 3, pp. 343–351, May 2017, doi: 10.1007/s10548-016-0540-0.
[33] I. P. Bodala, S. Kukreja, J. Li, N. V. Thakor, and H. Al-Nashash, "Eye tracking and EEG synchronization to analyze microsaccades during a workload task," in *Proc. 37th Annu. Int. Conf. IEEE Eng. Med. Biol. Soc. (EMBC)*, Aug. 2015, pp. 7994–7997, doi: 10.1109/EMBC.2015.7320247.
[34] F. Al-Shargie, U. Tariq, O. Hassanin, H. Mir, F. Babiloni, and H. Al-Nashash, "Brain connectivity analysis under semantic vigilance and enhanced mental states," *Brain Sci.*, vol. 9, no. 12, p. 363, Dec. 2019, doi: 10.3390/brainsci9120363.
[35] O. Hassanin, F. Al-Shargie, U. Tariq, and H. Al-Nashash, "Asymmetry of regional phase synchrony cortical networks under cognitive alertness and vigilance decrement states," *IEEE Trans. Neural Syst. Rehabil. Eng.*, vol. 29, pp. 2378–2387, 2021, doi: 10.1109/TNSRE.2021.3125420.
[36] I. P. Bodala, J. Li, N. V. Thakor, and H. Al-Nashash, "EEG and eye tracking demonstrate vigilance enhancement with challenge integration," *Frontiers Hum. Neurosci.*, vol. 10, p. 273, Jun. 2016, doi: 10.3389/fnhum.2016.00273.
[37] I. P. Bodala, N. I. Abbasi, Y. Sun, A. Bezerianos, H. Al-Nashash, and N. V. Thakor, "Measuring vigilance decrement using computer vision assisted eye tracking in dynamic naturalistic environments," in *Proc. 39th Annu. Int. Conf. IEEE Eng. Med. Biol. Soc. (EMBC)*, Jul. 2017, pp. 2478–2481, doi: 10.1109/EMBC.2017.8037359.
[38] N. A. Farha, F. Al-Shargie, U. Tariq, and H. Al-Nashash, "Improved cognitive vigilance assessment after artifact reduction with wavelet independent component analysis," *Sensors*, vol. 22, no. 8, p. 3051, Apr. 2022.
[39] F. M. Al-Shargie, O. Hassanin, U. Tariq, and H. Al-Nashash, "EEG-based semantic vigilance level classification using directed connectivity patterns and graph theory analysis," *IEEE Access*, vol. 8, pp. 115941–115956, 2020, doi: 10.1109/ACCESS.2020.3004504.
[40] F. Al-Shargie, T. B. Tang, and M. Kiguchi, "Assessment of mental stress effects on prefrontal cortical activities using canonical correlation analysis: An fNIRS-EEG study," *Biomed. Opt. Exp.*, vol. 8, no. 5, p. 2583, May 2017, doi: 10.1364/boe.8.002583.
[41] H. T. Wang, J. Smallwood, J. Mourao-Miranda, C. H. Xia, T. D. Satterthwaite, D. S. Bassett, and D. Bzdok, "Finding the needle in a high-dimensional haystack: Canonical correlation analysis for neuroscientists," *NeuroImage*, vol. 216, Aug. 2020, Art. no. 116749, doi: 10.1016/j.neuroimage.2020.116745.

[42] S.-M. Lee and S.-K. Lee, ''Psychoacoustical analysis and application of electroencephalography(EEG) to the sound quality analysis for acceleration sound of a passenger car,'' *Trans. Korean Soc. Noise Vibrat. Eng.*, vol. 23, no. 3, pp. 258–266, Mar. 2013, doi: 10.5050/ksnve.2013.23.3.258.
[43] A. Boudaya, B. Bouaziz, S. Chaabene, L. Chaâri, A. Ammar, and A. Hökelmann, ''EEG-based hypo-vigilance detection using convolutional neural network,'' in *Proc. Int. Conf. Smart Homes Health Telematics*. Cham, Switzerland: Springer, 2020, pp. 69–78, doi: 10.1007/978-3-030-51517-1.
[44] F. Pulvermuller, N. Birbaumer, W. Lutzenberger, and B. Mohr, ''High-frequency brain activity: Its possible role in attention, perception and language processing,'' *Prog. Neurobiol.*, vol. 52, no. 5, pp. 427–445, Aug. 1997.
[45] P. Zarjam, J. Epps, and F. Chen, ''Characterizing working memory load using EEG delta activity,'' in *Proc. 19th Eur. Signal Process. Conf.*, 2011, pp. 1554–1558.
[46] S. Jacobson and E. M. Marcus, *Neuroanatomy for the Neuroscientist*. New York, NY USA: Springer, 2008.
[47] M. Roohi-azizi, L. Azimi, S. Heysieattalab, and M. Aamidfar, ''Changes of the brain's bioelectrical activity in cognition, consciousness, and some mental disorders,'' *Med. J. Islamic Republic Iran*, vol. 31, p. 53, Sep. 2017.
[48] X. Liu, T. Chen, G. Xie, and G. Liu, ''Contact-free cognitive load recognition based on eye movement,'' *J. Electr. Comput. Eng.*, vol. 2016, pp. 1–8, Oct. 2016, doi: 10.1155/2016/1601879.
[49] M. Pomplun and S. Sunkara, ''Pupil dilation as an indicator of cognitive workload in human-computer interaction,'' in *Human-Centered Computing*. Boca Raton, FL, USA: CRC Press, 2019, pp. 542–546.
[50] P. van der Wel and H. van Steenbergen, ''Pupil dilation as an index of effort in cognitive control tasks: A review,'' *Psychonomic Bull. Rev.*, vol. 25, no. 6, pp. 2005–2015, Dec. 2018, doi: 10.3758/s13423-018-1432-y.
[51] A.-R. Mohammadi-Nejad, G.-A. Hossein-Zadeh, and H. Soltanian-Zadeh, ''Structured and sparse canonical correlation analysis as a brain-wide multi-modal data fusion approach,'' *IEEE Trans. Med. Imag.*, vol. 36, no. 7, pp. 1438–1448, Jul. 2017, doi: 10.1109/TMI.2017.2681966.
[52] M. Levine, ''Canonical correlational analysis,'' *Canonical Anal. Factor Comp.*, vol. 2, no. 6, pp. 12–36, 2011, doi: 10.4135/9781412983563.n1.
[53] V. Calhoun, T. Adali, G. Pearlson, and K. Kiehl, ''Neuronal chronometry of target detection: Fusion of hemodynamic and event-related potential data,'' in *Proc. IEEE Workshop Mach. Learn. Signal Process.*, Jun. 2014, pp. 239–244, doi: 10.1109/MLSP.2005.1532906.
[54] V. Calhoun, T. Adali, and J. Liu, ''A feature-based approach to combine functional MRI, structural MRI and EEG brain imaging data,'' in *Proc. Int. Conf. IEEE Eng. Med. Biol. Soc.*, Aug. 2006, pp. 3672–3675, doi: 10.1109/IEMBS.2006.259810.
[55] T. Harmony, ''The functional significance of delta oscillations in cognitive processing,'' *Frontiers Integrative Neurosci.*, vol. 7, pp. 1–10, Dec. 2013, doi: 10.3389/fnint.2013.00083.
[56] G. G. Knyazev, ''Motivation, emotion, and their inhibitory control mirrored in brain oscillations,'' *Neurosci. Biobehav. Rev.*, vol. 31, no. 3, pp. 377–395, Jan. 2007, doi: 10.1016/j.neubiorev.2006.10.004.
[57] F. L. Da Silva, ''Neural mechanisms underlying brain waves: From neural membranes to networks,'' *Electroencephalogr. Clin. Neurophysiol.*, vol. 79, no. 2, pp. 81–93, Aug. 1991, doi: https://doi.org/10.1016/0013-4694(91)90044-5.
[58] M. Plechawska-Wójcik, M. Tokovarov, M. Kaczorowska, and D. Zapała, ''A three-class classification of cognitive workload based on EEG spectral data,'' *Appl. Sci.*, vol. 9, no. 24, p. 5340, Dec. 2019, doi: 10.3390/app9245340.
[59] A. Holm, K. Lukander, J. Korpela, M. Sallinen, and K. M. I. Müller, ''Estimating brain load from the EEG,'' *Sci. World J.*, vol. 9, pp. 639–651, Jun. 2009, doi: 10.1100/tsw.2009.83.
[60] I. Seleznov, I. Zyma, K. Kiyono, S. Tukaev, A. Popov, M. Chernykh, and O. Shpenkov, ''Detrended fluctuation, coherence, and spectral power analysis of activation rearrangement in EEG dynamics during cognitive workload,'' *Frontiers Hum. Neurosci.*, vol. 13, pp. 1–16, Aug. 2019, doi: 10.3389/fnhum.2019.00270.
[61] P. Zarjam, J. Epps, F. Chen, and N. H. Lovell, ''Estimating cognitive workload using wavelet entropy-based features during an arithmetic task,'' *Comput. Biol. Med.*, vol. 43, no. 12, pp. 2186–2195, Dec. 2013, doi: 10.1016/j.compbiomed.2013.08.021.
[62] E. W. Anderson, K. C. Potter, L. E. Matzen, J. F. Shepherd, G. A. Preston, and C. T. Silva, ''Auser study of visualization effectivness using EEG and cognitive load,'' *Comput. Graph. Forum*, vol. 30, no. 3, pp. 791–800, 2011.

**NADIA ABU FARHA** received the B.Sc. degree in biomedical engineering from Hashemite University, Jordan, in 2015, the M.Sc. degree in biomedical engineering from the American University of Sharjah, UAE, in 2021, where she is currently pursuing the Ph.D. degree in biomedical engineering. Currently, she is a Physics Teacher with the Emirates National School, UAE. Her research interests include data mining, artifact removal, developing new classification methods, and neuroscience that focuses on the brain, its impact on behavior (stress, emotions, and alertness), and cognitive functions.

**FARES AL-SHARGIE** (Member, IEEE) received the B.S. and M.S. degrees in biomedical engineering from Multimedia University, Malaysia, and the Ph.D. degree in biomedical engineering from Universiti Teknologi PETRONAS, Malaysia. He has authored more than 30 journal and conference papers, one book, and one book chapter. He worked closely with several Biomedical Engineering Departments and Companies, including Hitachi Ltd. Research and Development Group, JAPAN, MBRSC, NASA, and SIRIUS. His current research interests include the assessment and mitigation of mental stress, sustained attention, deepfake, and emotions via, EEG, fNIRS neuroimaging modality, and eye tracking. He is a member of the Society of Functional Near-Infrared Spectroscopy.

**USMAN TARIQ** (Member, IEEE) received the M.S. and Ph.D. degrees from the Electrical and Computer Engineering Department, University of Illinois at Urbana–Champaign (UIUC), in 2009 and 2013, respectively. He was a Research Scientist at the Xerox Research Center Europe, Computer Vision Group, France. He is currently a Faculty Member with the Department of Electrical Engineering, American University of Sharjah (AUS), UAE. His research interests include computer vision, image processing, and machine learning, while facial expression recognition, and face biometrics.

**HASAN AL-NASHASH** (Senior Member, IEEE) is a Professor and the Former Director of the Biomedical Engineering Graduate Program, American University of Sharjah. He has authored of more than 100 journal and conference papers, six book chapters, and two issued U.S. patents. His research interests include neuroengineering, signal processing, microelectronics, cognitive vigilance, emotions assessment and enhancement, brain source localization, assessment of spinal cord and brain injuries, flexible implantable electrodes, and low power electronic devices. He led the effort to establish the biosciences and bioengineering academic programs and research at AUS. He received a number of awards and was the keynote and invited speaker at several conferences. He worked closely with several BME Departments and hospitals. He is currently the Vice Chair of the EMB Standards Committee (EMB-SC).